# Analysis of Oxide Reduction during Sintering of Cr-alloyed Steel Powder through Photoacoustic Spectroscopy Measurements

*Ola Bergman, Höganäs AB, SE-263 83 Höganäs, Sweden*
*Karin Frisk, Swerea KIMAB AB, SE-102 16 Stockholm, Sweden*
*Lars Nyborg, Chalmers University of Technology, SE-412 96 Göteborg, Sweden*

## Abstract

The usage of steel powders prealloyed with chromium in PM components for high performance applications is steadily increasing. Excellent mechanical properties are achieved with these powder grades, provided that the processing into components is accurately done. Photoacoustic spectroscopy (PAS) technique has been used here to study oxide reduction during sintering in $90N_2/10H_2$ atmosphere of test specimens based on 3%Cr-0.5%Mo prealloyed powders with 0.5% C added. Results from performed reduction trials show that Fe oxides on the powder surfaces are removed by $H_2$ reduction early in the heating stage of the process. Carbothermal reduction is the main mechanism for reduction of stable Cr-containing oxides from 900°C and above. Efficient Cr oxide reduction requires a sintering temperature of at least around 1200°C. Therefore, small oxide particles remain in the material after sintering at 1120°C for 30 minutes. However, such oxides have earlier been shown to have no significant influence on mechanical properties.

## Introduction

The development of Cr-alloyed steel powder grades for structural PM components has been driven by the high and volatile prices in recent years of the commonly used alloying elements Mo and Ni. Water-atomized powders prealloyed with 1.5-3% Cr and 0.2-0.5% Mo have now been available for some years and using these materials is a cost effective way to reach the mechanical properties needed for high performance applications [1]. Well-controlled sintering is a prerequisite for successful processing of Cr-alloyed powders due to the oxidation sensitivity of Cr. Hence, sintering atmospheres with low oxygen content must be used in order to have reducing conditions [2]. Furthermore, an appropriate temperature cycle should be applied to ensure that sufficient reduction of oxides on the powder surfaces occurs in the process. Components with high mechanical performance can be obtained after sintering at a temperature (1120°C) typically used in conventional mesh belt production furnaces, but to exploit the full potential of the Cr-alloyed materials higher sintering temperatures must be used [3]. The aim of the investigation presented in this article was to study oxide reduction mechanisms during sintering of Cr-alloyed steel powder and, thereby, gain better knowledge on how to optimize a sintering process for this type of material.

Surface oxides on the Cr-alloyed steel powder grades have a heterogeneous structure consisting of Cr-rich particulate compounds (size up to 0.2 μm) surrounded by a thin (6-7 nm) continuous Fe oxide layer [4]. The possibility to reduce these oxides is determined by their thermodynamic stability, which depends on alloy composition of the steel, temperature, and oxygen pressure in the surrounding atmosphere. Figure 1 shows oxide phases appearing at thermodynamic equilibrium in a Fe-3%Cr alloy for different temperatures and fixed oxygen partial pressure. Accordingly, $Cr_2O_3$ is the most stable oxide phase in such an alloy, followed by the spinel oxide $FeCr_2O_4$, and relatively high temperatures are required to have reducing conditions for these oxides at the given oxygen pressure. The iron oxide phases (FeO, $Fe_3O_4$, $Fe_2O_3$) are less thermodynamically stable and may be reduced at lower temperatures.

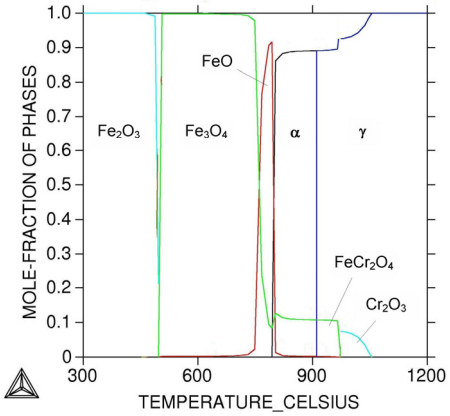



**Figure 1.** Mole fraction of phases versus temperature for Fe-3%Cr alloy in equilibrium with atmosphere where $p_{O2} = 10^{-19}$ atm (from Thermo-Calc).

Besides favourable thermodynamic conditions, reduction media have to be available for removal of the oxides. In the sintering process, metal oxide ($M_xO_y$) reduction occurs either through interaction with $H_2$ in the atmosphere according to reaction (1), or via carbothermal reduction through interaction with C in the material according to reactions (2) and (3).

$$M_xO_y(s) + yH_2(g) \rightarrow xM(s) + yH_2O(g) \quad (1)$$

$$M_xO_y(s) + yC(g) \rightarrow xM(s) + yCO(g) \quad (2)$$

$$M_xO_y(s) + yCO(g) \rightarrow xM(s) + yCO_2(g) \quad (3)$$

The carbothermal reduction starts in accordance with reaction (2) when the temperature is high enough to activate the carbon in the powder compact. However, as soon as CO becomes available reaction (3) will be the dominating reduction mechanism, and regeneration of CO is ensured at high temperatures by the Boudouard reaction:

$$C(s) + CO_2(g) \rightarrow 2CO(g) \quad (4)$$

The reactions above show that oxide reduction during sintering may be studied by monitoring concentrations of the gaseous reaction species $H_2O$, CO and $CO_2$ in the process atmosphere. In earlier investigations of oxide reduction in Cr-alloyed PM grades, mass spectrometry and dilatometry have been used to study deoxidation during slow heating of compacts in vacuum or He atmosphere [5-7]. In the present investigation, PAS technique for high precision gas analysis was applied in slow heating as well as simulated sintering trials in $N_2/H_2$ atmosphere with pressed specimens based on Cr-alloyed steel powder.

## Experimental procedure

The water-atomized powder grade Astaloy CrM, which is prealloyed with 3% Cr and 0.5% Mo, was used as test material. Oxygen content of the utilized powder sample was 0.15%. This powder was mixed with 0.5% graphite (Kropfmühl UF4) and 0.6% lubricant (Kenolube P11). Cylindrical test specimens (diameter 25 mm, height 20 mm) were produced by uniaxial compaction of the powder mix with a compaction pressure of 600 MPa. Dewaxing was done by heat treating the test specimens for 30 minutes at 700°C in $75H_2/25N_2$ atmosphere.

| Density (g/cm$^3$) | C (%) | O (%) |
|---|---|---|
| 6.94 | 0.50 | 0.20 |

**Table 1.** Test specimen properties after dewaxing.

An experimental set-up consisting of a tube furnace connected to a PAS instrument for gas analysis was used for oxide reduction trials. Three different reduction trials were performed with one specimen in each trial (see Table 2). A very low heating rate was applied in the first trial, while faster heating was used in the other two trials in order to simulate realistic sintering cycles. In all trials, a constant flow of high purity (dew point ~ -60°C) $90N_2/10H_2$ atmosphere was running through the furnace tube (inner diameter 35 mm) at a rate of 5 litres per minute. Concentrations (>1 ppm) of $H_2O$, CO, $CO_2$ and $CH_4$ in the outgoing gas from the furnace were analysed by the PAS instrument throughout the experiments. The time between sample collections by the PAS instrument was about 60 seconds.

| Trial # | Temperature cycle | Atmosphere |
|---|---|---|
| 1 | Slow heating (5°C/min) to 1300°C + 10 min isotherm | $90N_2/10H_2$ |
| 2 | Simulated sintering cycle: 1120°C for 30 min | $90N_2/10H_2$ |
| 3 | Simulated sintering cycle: 1250°C for 30 min | $90N_2/10H_2$ |

**Table 2.** Temperature cycles applied in the oxide reduction trials. Sintering temperature was reached after about 68 minutes in both simulated sintering cycles.

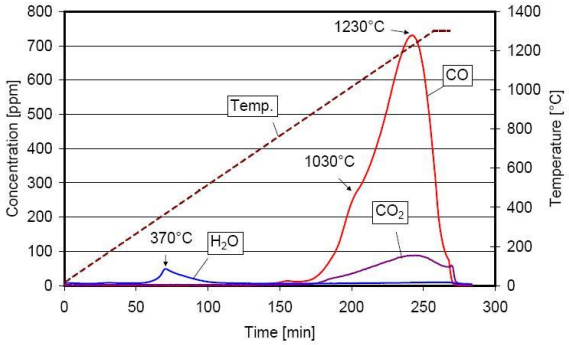
After the reduction trials, cross sections of the test specimens were examined by light optical microscopy (LOM). Bulk analyses of oxygen and carbon contents were done in LECO instruments.

**Results**

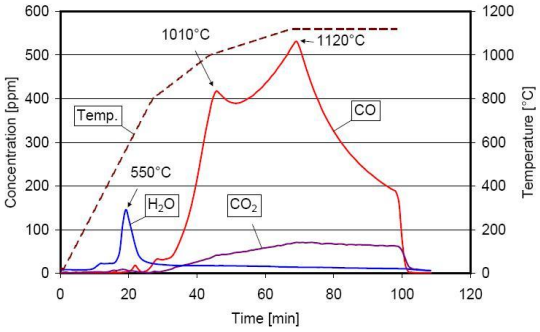
Results from the PAS analysis of gas concentrations in the reduction trials are presented in Figure 2. The $CH_4$ concentration was low (<10 ppm) throughout all three trials and is not included in the graphs.

In the slow heating trial, there is an $H_2O$ peak starting at around 300°C and with a maximum value at 370°C, which corresponds to $H_2$ reduction of easily reduced iron oxides. After this peak has declined the $H_2O$ concentration stays below 10 ppm the rest of the trial. The CO concentration starts to increase at about 700°C, which marks the onset of carbothermal reduction of more stable oxides. There is a small CO peak just below 800°C and at around 850°C the CO concentration increases sharply to form a large peak at 1230°C. This peak also has a shoulder at about 1030°C. The $CO_2$ concentration increases steadily from about 850°C to form a peak at around 1230°C, in conjunction with the much larger CO peak.

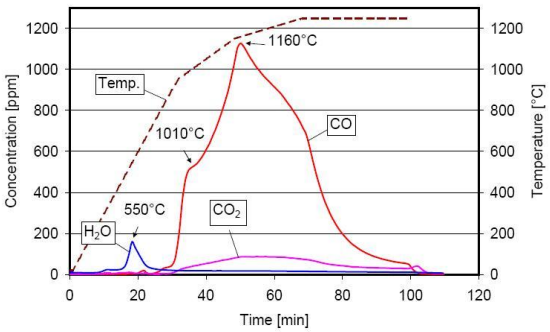
The $H_2O$ concentration curves from the two simulated sintering trials are almost identical. There is a single peak with maximum value at about 550°C, corresponding to hydrogen reduction of iron oxides, where after the $H_2O$ concentration slowly decreases from 20 ppm to 10 ppm at the end of the trial. A small CO peak appears in both trials in connection with the $H_2O$ peak. In the 1120°C sintering trial, CO formation due to carbothermal oxide reduction starts at around 750°C and there is a relatively small CO peak at 815°C. After that, the CO concentration increases rapidly and peaks at 1010°C followed by a second peak as the sintering temperature 1120°C is reached. The CO content decreases continuously during the hold time at 1120°C but the concentration is still relatively high (~190 ppm) at the end of the isotherm. Also in the 1250°C sintering trial, CO formation due to carbothermal reduction appears at around 750°C. The CO concentration increases slowly until 900°C after which the concentration increases rapidly to a peak value at 1160°C, with a peak shoulder at around 1010°C. When the sintering temperature 1250°C is reached, the CO content starts to decrease rapidly reaching a relatively low level (~50 ppm) at the end of the isotherm. Increase in $CO_2$ concentration starts in both sintering trials between 800°C and 850°C. In the 1120°C trial, $CO_2$ increases steadily until the sintering temperature is reached, whereupon the concentration stays more or less constant at ~70 ppm during the isotherm. In the 1250°C trial, $CO_2$ increases until 1160°C where the concentration levels out at ~85 ppm until 1220°C, and then the concentration decreases slowly until the end of the isotherm.




*Trial 1: Slow heating to 1300°C.*



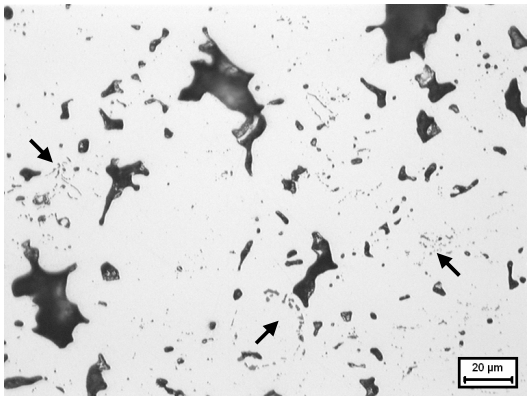

*Trial 2: Sintering at 1120°C for 30 min.*



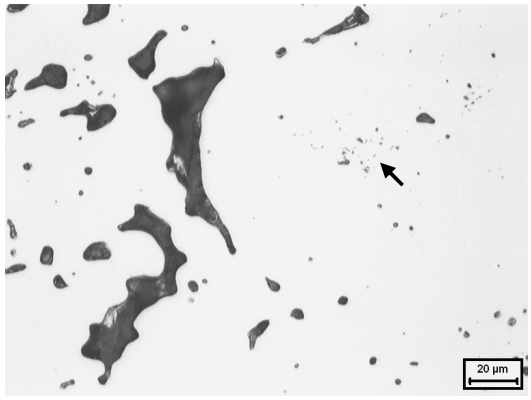

*Trial 3: Sintering at 1250°C for 30 min.*

**Figure 2.** Results from gas analysis by PAS in oxide reduction trials on test specimens of Astaloy CrM + 0.5% C in $90N_2/10H_2$ atmosphere.

Bulk analyses of oxygen contents in the test specimens show that the material contains 0.099% O after the 1120°C sintering trial and 0.014% O after the 1250°C sintering trial. This large difference in oxygen content is also visible in the microstructures of the specimens (see Figure 3). There are small oxide particles (up to a few μm in size) throughout the structure of the 1120°C sintered material, both along former powder particle boundaries and inside the former powder particles, while the structure of the 1250°C sintered material is very clean and only contains few traces of oxides. The specimen from the slow heating trial has similar structure as the 1250°C sintered material and also low bulk oxygen content (0.021% O).




*Trial 2: Sintering at 1120°C for 30 min.*




*Trial 3: Sintering at 1250°C for 30 min.*

**Figure 3.** As-polished microstructures in test specimens of Astaloy CrM + 0.5% C after oxide reduction trials in $90N_2/10H_2$ atmosphere. Oxides in the structures are marked by arrows.

The test specimen from the 1120°C sintering trial has highest carbon content (0.43% C) and lowest density (7.02 g/cm$^3$). The specimens from the other two trials are comparable in both carbon content and density, with 0.36% C and 7.08 g/cm$^3$ for the 1250°C sintered material, plus 0.38% C and 7.09 g/cm$^3$ for the material from the slow heating trial.

## Discussion

The thermodynamic calculation results presented in Figure 1 give a stability ranking for oxide phases in the investigated material. This stability ranking may be used to determine which oxides the different reduction peaks correspond to in the gas concentration curves from the reduction trials. However, agreement between the results in Figure 1 and the experiments cannot be expected regarding reduction temperatures, since the oxygen partial pressure is not constant in the reduction trials. In a process gas with fixed dew point, $p_{O2}$ will increase with temperature in accordance with the gas equilibrium reaction $H_2 + ½O_2 = H_2O$. The $N_2/H_2$ atmosphere used in the trials has a $H_2O$ level of ~10 ppm, which means that $p_{O2}$ is below the value ($10^{-19}$ atm) used in the calculations up to temperatures over 1250°C.

In the slow heating trial, the $H_2O$ peak at 370°C should represent reduction of the easily reduced iron oxides $Fe_2O_3$ and $Fe_3O_4$. The small CO peak at around 800°C should correspond to FeO reduction, which is supported by earlier reports on the necessary temperature for carbothermal reduction of this oxide [8]. Remaining is reduction of the Cr-containing oxides, which is represented by the large CO peak starting at about 850°C. The peak shoulder at 1030°C is attributed to transition from Fe-Cr oxide reduction to Cr oxide reduction. Reduction maximum at 1230°C for the most stable oxide is in line with results from previous studies on oxide reduction of Cr-alloyed steel powder compacts [5,6].

Corresponding reduction peaks to those in the slow heating trial are found in the two simulated sintering trials. Accordingly, hydrogen reduction of $Fe_2O_3/Fe_3O_4$ occurs in the initial heating stage, represented by the $H_2O$ peaks at around 550°C. The carbothermal reduction is initiated at about 750°C and there is some FeO reduction before reduction of the Cr-containing oxides starts at around 900°C, as marked by the sharp increases in CO concentration at that temperature. The change in the CO curves just above 1000°C indicates that the Fe-Cr oxide reduction declines and that the Cr oxide reduction starts, although the decrease in heating rate at that temperature should also influence. In the 1120°C sintering trial, there is a drop off in CO concentration when the sintering temperature is reached, showing that the Cr oxide reduction progresses rather slowly during the isotherm. In the 1250°C sintering trial, the peak in CO concentration at 1160°C should be a consequence of the decrease in heating rate at that temperature. However, there are still high CO concentrations up to the sintering temperature indicating effective Cr oxide reduction, and the rapid decline in CO during the isotherm should be due to that most oxides are reduced at this point.

The fact that efficient oxide reduction is achieved in the 1250°C sintering trial is verified by the low oxygen content in the material afterwards and the basically oxide free microstructure of the sintered specimen. The specimen from the 1120°C sintering trial, on the other hand, has about ~0.1% residual oxygen and many small oxide particles are visible in the microstructure. These should be Cr-rich oxides that originate either from particulate compounds on the powder surfaces or from small oxides inside the powder particles. Hence, the kinetics for Cr oxide reduction is not good enough at 1120°C. As the slow heating trial shows, the Cr oxide reduction becomes much more efficient at temperatures around 1200°C and above. It has also been demonstrated in a previous investigation that nearly complete oxide reduction is achieved when sintering Cr-alloyed PM steels at 1200°C [3].

Although some oxides remain in the Cr-alloyed material after sintering at 1120°C, the microstructure demonstrates that there are well-developed sinter necks between powder

particles. This is ensured by the removal of the continuous Fe oxide layer on the powder particles early in the heating stage of the sintering process, as shown in the reduction trials. Consequently, the Cr oxide particles do not have any significant effect on the bonding between particles during sintering, and it is clear that high mechanical performance is attainable with the Cr-alloyed powder grades after 1120°C sintering [1]. However, by sintering at temperatures where complete oxide reduction occurs, the mechanical properties of Cr-alloyed PM steel can be boosted to even higher levels [1,3].

It is evident from the reduction trials that carbothermal reduction, represented by the large CO peaks, is the main mechanism for oxide reduction in the sintering process. Hydrogen-assisted reduction is detected during heating, but there is no $H_2O$ formation above around 700°C. Yet, the increases in $CO_2$ concentration obtained in the trials at higher temperatures might be an indication of oxide reduction by $H_2$, since any $H_2O$ formed according to reaction (1) is likely to react with CO and form $CO_2$ according to the water-gas shift reaction:

$$CO(g) + H_2O(g) \rightarrow CO_2(g) + H_2(g) \qquad (5)$$

The test specimens used in the investigation were somewhat oxidized in the dewaxing process prior to the reduction trials. In spite of this, the specimen characteristics after the simulated sintering trials are comparable to what is usually obtained in corresponding sinterings of Cr-alloyed powder grades. Hence, this oxidation did not have any significant influence on the overall reduction processes in the performed experiments.

## Conclusions

Conclusions regarding sintering of pressed compacts (density ~7.0 g/cm$^3$), based on 3%Cr-0.5%Mo prealloyed steel powder with 0.5% C added, in $90N_2/10H_2$ atmosphere:

- Iron oxides on the powder surfaces are reduced by $H_2$ early in the heating stage of the process. Carbothermal reduction by C in the material starts at around 750°C, and is the dominating mechanism for removal of stable Cr-containing oxides at higher temperatures.
- Cr oxide reduction is initiated at around 1000°C, but for efficient reduction of this oxide a temperature of about 1200°C or above is required.
- Small oxide particles, typically of μm size, remain in the material after sintering at 1120°C for 30 minutes due to insufficient kinetics for Cr oxide reduction. Such particles are not detrimental for the mechanical properties of the sintered component.
- Sintering at 1250°C for 30 minutes leads to practically complete reduction of oxides, leaving only traces of oxides in the material.

## References


[1] U. Engström, D. Milligan, A. Klekovkin: Advances in Powder Metallurgy & Particulate Materials, 2006, Vol. 2, Part 7, pp. 21-32.
[2] O. Bergman: Powder Metallurgy, 2007, Vol. 50, No. 3, pp. 243-249.
[3] O. Bergman, B. Lindqvist, S. Bengtsson: Materials Science Forum, 2007, Vols. 534-536, pp. 545-548.
[4] H. Karlsson, L. Nyborg, S. Berg: Powder Metallurgy, 2005, Vol. 48, pp. 51-58.
[5] H. Danninger, C. Gierl, S. Kremel, G. Leitner, K. Jaenicke-Roessler, Y. Yu: Powder Metallurgy Progress, 2002, Vol. 2, pp. 125-140.
[6] S. Kremel, H. Danninger, Y. Yu: Powder Metallurgy Progress, 2002, Vol. 2, pp. 211-221.
[7] H. Danninger, C. Xu: Proc. of Euro PM2003, Valencia, Spain, October 2003, EPMA, Vol. 1, pp. 269-274.
[8] S. C. Mitchell, A. Cias: Powder Metallurgy Progress, 2004, Vol. 4, pp. 132-142.